International Journal of Advanced Trends in Engineering and Management (IJATEM)
Vol. 1(06), November 2022, pp. 25-33
Article Title: **Brain Cancer Area Segmentation Using Intelligent Fuzzy Based Approach**

Brain Cancer Area Segmentation Using Intelligent Fuzzy Based Approach

P. Kavitha
Department of Electrical and Electronics Engineering, Government College of Engineering, Tirunelveli, Tamilnadu, India.
kavitha.paulsamy6@gmail.com

ABSTRACT
Brain cancer is among the most dangerous tumors for patients of all ages, and radiologists find it challenging to determine its grade in automated diagnosis and health monitoring systems aiding radiologists in performing better diagnostic analysis, numerous deep learning-based methods for Brain Cancer Classification (BTC) have recently been presented in the literature. In this paper, an Intelligent Fuzzy Based Approach is adopted for the detection of brain cancer. The input images are first pre-processed using the Weiner filter, then the segmentation of the brain cancer image is done used by the Fuzzy C Means algorithm. From each segmented tissue, related features are then extracted using the Gray Level Co-occurrence Matrix (GLCM) method, and the features are chosen using the adaptive threshold method. In in order to improve quality and accuracy. Adaptive Neuro-Fuzzy Inference System (ANFIS) are utilized for classification which in turn effectively determines the presence or absence of brain cancer. In this paper, the results are adapted from the MATLAB software.
Keywords: Brain cancer, Weiner filter, GLCM, FCM.

1 Introduction

The different cell types that make up the human body. The human brain is a sensitive and highly specialized organ. One of the most critical diseases that has to be treated worldwide is brain cancer [1]. Malignant brain cancer can occur as a result of abnormal brain cell growth, which is the primary cause of most brain diseases [2]. Early detection of brain metastases increases cancer patient survival, as image-guided radiosurgery is the most widely used treatment [3]. To remove the salt-and-pepper noise, use an Iterative Mean Filter (IMF) [4]. The resultant grayscale image has salt and pepper noise removed using median filtering. The median of that pixel's intensity values immediate vicinity is used to replace the value of the center pixel. The median filter has the disadvantage of being more complex and time-consuming than the mean filter [5]. To overcome the shortcomings of existing filter the proposed work utilized weiner filter concept for image denoising. Furthermore, an image segmentation algorithm called the OTSU method (OTSU) uses a global adaptive binarization threshold. The simplicity and high accuracy of the OSTU approach are advantages, but OTSU segmentation has a low real-time efficiency [6]. There are different methods, and one of the most used clustering algorithms is k-means. Unsupervised K-means clustering is employed to segment the interest area from the background. The disadvantage of k-means is that it requires a partial stretching enhancement to be used on the image before it can be used [7]. To overcome the shortcomings of existing method the proposed work utilized FCM concept for image segmentation. Furthermore, it has long been known that the principal component analysis (PCA) is a useful and for hyper spectral image (HSI) processing and analysis tasks, an efficient preprocessing step [8]. The disadvantage of PCA is the low interpretability of its principal components. The widely used SURF feature point extraction method maintains the robustness and accuracy of SIFT feature point extraction while speeding up the process [9]. High dimension of feature descriptor, large amount of computation, and poor matching accuracy are drawbacks. To overcome the shortcomings of existing method the proposed work utilized GLCM concept for Feature Extraction. Using random forest will enable for a significant reduction in energy consumption while retaining high classification accuracy (MSLM-RF). Additionally, after fusing spectral and spatial features, the proposed MSLM-RF (multiscale maximum filters) uses random forests to classify data [10]. Because it uses multiple decision trees to make prediction, this algorithm performs considerably slower than other classification algorithms. The Support Vector Machine (SVM) classifier is initially widely used to filter out irrelevant images as a category prediction for database and query images in order to reduce the search space for similarity matching [11]. The SVM algorithm is not well suited to handle large data sets. SVM performs poorly when there is more noise in the data set. To overcome the shortcomings of existing classifier the proposed work utilized ANFIS classifier. The primary objective of this research is to review and analyze various research papers in order to identify various filters, segmentation methods, and algorithms for brain cancer area segmentation.

2 Recent Works

Yue Zhang et al [2020] [12] proposed one of today's most dangerous diseases and a major manifestation of several cerebrovascular diseases. Deep learning has rapidly grown recently and offers a potential for segmenting medical images is great. In contrast to most deep learning-based segmentation methods, which only utilise magnetic resonance (MR) images as the input, a novel method for segmenting stroke lesions called multi-inputs UNet (MI-UNet) that incorporates information about brain parcellation, including grey matter (GM), white matter (WM), and the lateral ventricle (LV), is proposed and validated in this paper. A dataset of 229 T1-weighted MR images is used to validate the effectiveness of the proposed workflow. Both in 2D and 3D settings, the proposed MI-UNet performed significantly better than UNet.

Yongjin Zhou et al [2019] [13] proposed for medical diagnosis, prognosis, surgical planning and, the extent and location of lesions caused on by chronic stroke are critical. The encoder-decoder structure has recently shown excellent potential in the area of medical picture segmentation due to the rapid growth of 2D and 3D convolutional neural networks. While the

3D CNN suffers with high computational resource demands, the 2D CNN dismisses the 3D information in medical images. The proposed architecture improves 2D networks in terms of segmentation performance although 3D networks take less time to compute. Additionally, we provide the Enhance Mixing Loss (EML) loss function to solve the issue of data imbalance between negative and positive samples for network training. Three different methods have been tested against ATLAS dataset method.

Hyunkwang Lee et al [2019] [14] proposed to With improvements in deep learning and machine learning, computerised medical diagnoses that can inform clinical decision-making may one day be used. How these algorithms produce predictions from the input data, however, remains a black box. Large, superior training datasets are additionally required for high-performance deep learning. Here, the development detects the deep-learning system has five distinct forms of acute intracranial haemorrhage (ICH) from unenhanced head computed CT data is presented. In two separate test datasets with 200 cases each (sensitivity: 98%, specificity: 95%) and 196 cases each (sensitivity: 92%, specificity: 95%), the system performed similarly to experienced radiologists, while only employing a dataset of 904 examples for algorithm training.

Murtadha D. Hssayeni et al [2020] explained Intracranial haemorrhages (ICH) may result from traumatic brain injury. When treating ICH in a timely manner, accuracy in diagnosis and treatment are important, it could cause disability or death. However, the availability of a skilled radiologist is essential in this process to gather 82 CT scans of people who had suffered traumatic brain injuries. After that, two radiologists in consensus manually defined the ICH zones in each slice. The dataset is freely available online via the PhysioNet repository for upcoming analysis and comparisons. The primary objective of this study is to publish the dataset; however, a FCN, known as U-Net, is implemented to fully-automatically segment the CT scans' ICH regions. For the ICH segmentation, the method showed a Dice coefficient of 0.31 based on 5-fold cross-validation.

Xinfeng Liu et al [2019] [16] explained the capability to facilitate accurate surgical planning and stroke diagnosis. The segmentation of biomedical images has shown encouraging progress using existing deep neural networks, including U-net. The segmentation of stroke lesions still faces various challenges, such as dealing with fuzzy lesion boundaries, diverse lesion locations, and variable lesion scales. A deep encoder-decoder neural network working end to end is generally used in the proposed method. The cross connection between the encoder and the decoder ensures the feature mapping's high resolution.

3 Proposed Work Explanation

In this paper The CT image is used as the input data for this system. The input image is pre-processed with weiner filter for eliminating the noise. After pre-processing, the noise removed image is fed into the segmentation block for segmenting the image into several segments for further process. In this system, FCM clustering method is used. The feature extraction technique is used to process the segmented regions in order to extract various features and select the necessary features to assist classification. The GLCM, method is employed in this paper to extract and select features. In order to effectively classify the image, the final step includes selecting the chosen features into the ANFIS classifier and the block diagram is shown in Figure 1.

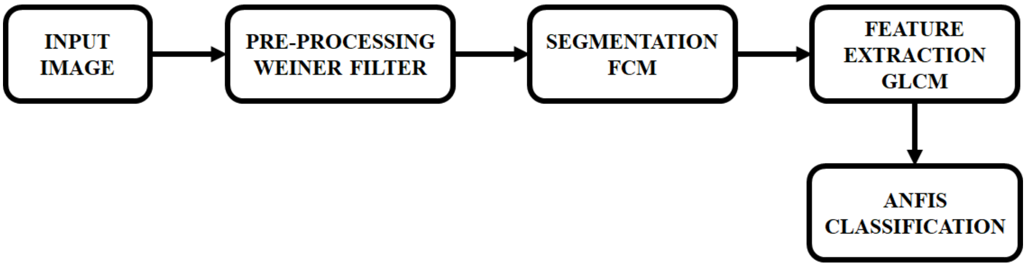

Figure 1: *Block Diagram*

3.1 Preprocessing Using Weiner filter

In regards of MSE, Wiener filtering is the best filter because it reduces the overall MSE while inverse filtering and noise smoothing are being used. This filter provides a linear estimate of the original image. The Wiener filter will remove additive noise while also inverting the obscuring. It is better to use a Wiener filter. The best way to rebuild a noisy signal in order to get a direct estimation of the first picture is to use Wiener filtering, which is a general technique. The skilled radiologist verified that the structure of the mammographic image is not altered by this filter. and instead improves visibility based on the psycho-visual criterion. A wiener filter's objective is to minimize the mean square error as much as possible.

3.2 Segmentation Using FCM

In the same way that the K-means algorithm compares every pixel's RGB value to the cluster center, the FCM method does the same. According to the fuzzy rule, a pixel's membership values for all clusters must be 1. The likely that a pixel belongs to a cluster as the membership value increases. By minimizing an objective function as shown in equation 1, the FCM clustering is obtained

$$J_m = \sum_{i=1}^{M} \sum_{j=1}^{C} u_v^m \parallel x_i - c_j \parallel^2 \qquad ,1 \le m < \infty \qquad (1)$$

Where u_{ij} is the degree of membership of x_i in the cluster j, m is any real number greater than 1, , c_j is the d-dimension center of the cluster, x_i is the ith of d-dimensional measured data, ||*|| is any norm expressing the similarity between any measured data and the center.

Equation 2 is employed to get the centroid of the k_{th} cluster

$$v_k = \frac{\sum_{i=1}^{n} \mu_{ik}^m \, p_i}{\sum_{i=1}^{n} \mu_{ik}^m} \qquad (2)$$

The fuzzy membership table is calculated using the original equation 3.

$$\mu_{ik} = \frac{1}{\sum_{i=1}^{c}\left(\frac{|p_i - v_k|}{|p_i - v_i|}\right)^{\frac{2}{m-1}}} \tag{3}$$

The clustering of colour images in the RGB colour space has been extended to the capabilities of this algorithm. As a result, equation 1's calculation of the Euclidean distance between pi and v_k is modified in equation 4 to take RGB colours incorporate.

$$|p_i - v_k| = \sqrt{\sum_{i=1}^{n}(p_{iR} - v_{kR})^2} + (p_{iG} - v_{kG})^2 + (p_{iB} - v_{kB})^2 \tag{4}$$

3.3 Feature Extraction Using GLCM

The statistical texture features are extracted in this research using first order statistics and second order texture GLCM. Only the first three features skewness, mean and standard deviation are computed, while the second order namely homogeneity, entropy, energy, contrast and correlation. Energy measures how smooth an image is. Lower values are used for images with high values and low contrast, are used for images with high contrast. Contrast measures local level variations. The homogeneity in the GLCM measures how evenly distributed the elements are. It has a range of 0 to 1. Entropy gives the randomness measure. Calculating the probability that an adjacency relationship will occur between two pixels at a specific distance and angular orientation is the method used to derive two-order statistics. The Gray Level Co-occurrence Matrix is the name of this method.

Energy, which is stated in equation 5 as the size of the pair's co-occurrence matrix concentration at a given grey intensity.

$$Energy = \sum_{i=1}^{L}\sum_{i=1}^{L} p(i,j)^2 \tag{5}$$

The image has a high contrast value if the image matrix's primary diagonal is a far distance away. Equation 6 gives a definition of contrast.

$$Contrast = \sum_{i}^{L}\sum_{j}^{L}|i-j|^2\, p(i,j) \tag{6}$$

The homogeneity of an image is represented on a grey scale level by homogeneity. Equation 7 gives a definition of homogeneity.

$$Homogenity = \sum_{i=1}^{L}\sum_{j=1}^{L}\frac{p(i,j)^2}{1+(i-j)^2} \tag{7}$$

Entropy shows the irregularity of the size and shape. Entropy calculates image information, which is defined in equation 8, measures information lost from a transition signal.

$$Entropy = \sum_{i=1}^{L}\sum_{1=1}^{L} p(i,j)\big(-In\, p(i,j)\big) \tag{8}$$

Correlation is employed to represent the linear dependence of the grey currency matrix in the image. Equation 9 can be used to define it.

$$Correalation = \sum_{i=1}^{L}\sum_{j=1}^{L}\frac{(i-\mu_i)(j-\mu_i)p(i,j)}{\sigma_i\sigma_j} \tag{9}$$

Figure 2 represents the flow chart of FCM.

International Journal of Advanced Trends in Engineering and Management (IJATEM)
Vol. 1(06), November 2022, pp. 25-33
Article Title: Brain Cancer Area Segmentation Using Intelligent Fuzzy Based Approach

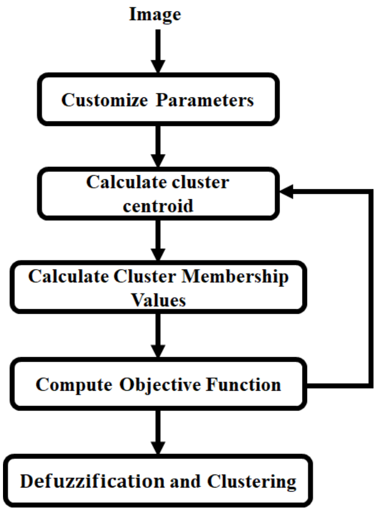

Figure 2: *Flowchart for FCM*

3.4 ANFIS Classifier

The classification of brain images as abnormal or normal employed several standard classifiers, including support neural networks, vector classifiers, etc. In this paper ANFIS classifier were used. Five hidden layers with an input and output layer make up an ANFIS classifier with multiple layers. As shown in Figure 3, a multi-layer ANFIS classifier was used in this paper to classify brain images as either normal or abnormal. Both training and testing are using the same architecture. The trained features from the normal images were given to X of the ANFIS architecture in the classifier's training mode, whereas the trained features from the abnormal images were given to Y. The test brain image's extracted features were given to the ANFIS classifier as input during the test or classification mode. Five hidden layers were finally set up to provide the better classification rate after testing hidden layers with different numbers of neurons.

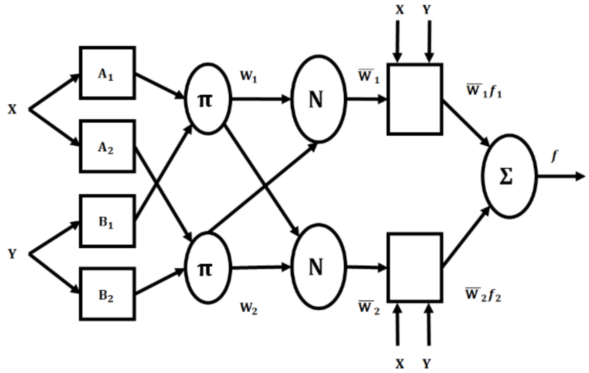

Figure 3: *ANFIS architecture.*

4 Results and Discussion

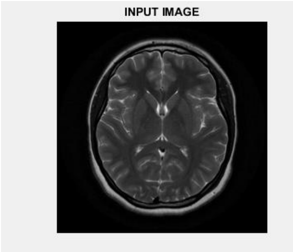

Figure 4: *Input image*

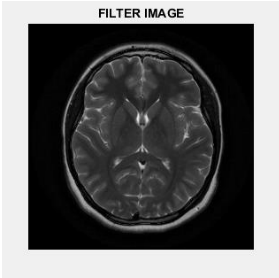

Figure 5: *Filter image*

The original input image to be processed is shown in Figure 4. The noise free filtered output using weiner filter is depicted in Figure 5.

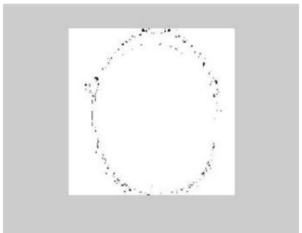

Figure 6: *Segmentation image*

	1	2	3	4	5	6	7
1	0.3343	1.0087e+03	1.2424e+03	0.0701	420.9915	0.2798	116.9317
2	0.3896	890.2566	5.2527e+03	0.2300	1.5239e+03	0.3682	139.4689
3	0.5598	1.2770e+03	1.3867e+04	0.4519	4.3432e+03	0.5669	147.2435
4	0.7049	1.4834e+03	2.8059e+04	0.7571	9.2935e+03	0.6934	169.6420
5	0.8854	1.5671e+03	5.1101e+04	1.1239	1.7405e+04	0.8754	185.9565
6	1.0020	2.0161e+03	8.1582e+04	1.5865	2.7694e+04	1.0062	198.7998
7	1.1524	2.2434e+03	1.2556e+05	2.1186	4.2170e+04	1.1619	222.9979
8	1.2847	2.4805e+03	1.8140e+05	2.7322	6.0482e+04	1.3089	237.4417
9	1.4185	2.6748e+03	2.5152e+05	3.4342	8.4046e+04	1.4529	251.8180
10	1.5843	2.9875e+03	3.4530e+05	4.2020	1.1479e+05	1.6368	273.6229
11	1.7582	3.2977e+03	4.5778e+05	5.0328	1.5272e+05	1.8179	296.5024
12	1.8500	3.3989e+03	5.6832e+05	5.9744	1.9100e+05	1.8985	310.2216
13	2.0362	3.7260e+03	7.2847e+05	6.9737	2.4523e+05	2.0850	333.7482
14	2.1751	3.9621e+03	8.9871e+05	8.0498	3.0189e+05	2.2237	354.4831
15	2.2640	4.0738e+03	1.0744e+06	9.2337	3.6022e+05	2.3160	364.5091
16	2.3801	4.2429e+03	1.2894e+06	10.5127	4.3135e+05	2.4382	380.4103
17	2.4855	4.3900e+03	1.5259e+06	11.8964	5.1005e+05	2.5466	395.2024
18	2.6289	4.6030e+03	1.8173e+06	13.3614	6.0639e+05	2.6971	414.8882
19	2.7580	4.7848e+03	2.1286e+06	14.9200	7.1129e+05	2.8244	432.9739
20	2.9253	5.0494e+03	2.5008e+06	16.5507	8.3831e+05	2.9921	454.5067
21	3.1076	5.3656e+03	2.9232e+06	18.2442	9.8322e+05	3.1737	477.8582

Figure 7: *Features Extraction*

The preprocessed output segmented using FCM is shown in Figure 6 indicating the area affected. The features extracted utilizing GLCM approach in segmented output image is shown in Figure 7. Effective classification of brain cancer performed using ANFIS classifier is shown in Figure 8.Its indicating the type of cancer affect. It is observed that with the propose work, the brain image classified is affected with benign.

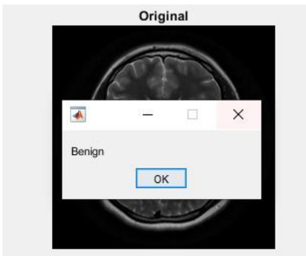

Figure 8: *Output image*

5 Conclusion

In this paper, an efficient method for detecting brain tumors is put presented. It makes use of different image processing stages to identify the tumor in the input brain CT images. In order to reduce the impulsive noises in the input CT pictures, the weiner filter is used. The preprocessing and segmentation of pictures are done using the FCM segmentation technique, respectively. The GLCM is applied to extract the features, and the ANFIS approach is applied to classify the images. Additionally, the suggested approach performs better than the previous methods and is effective.

References

1. Erkal Begüm; Selen Başak; Alper Çiloğlu; Duygu Dede Şener, Year: 2020, "Multiclass Classification of Brain Cancer with Machine Learning Algorithms," 2020 Medical Technologies Congress (TIPTEKNO), pp. 1-4.

2. Musallam Ahmed S; Ahmed S. Sherif; Mohamed K. Hussein, Year: 2022, "A New Convolutional Neural Network Architecture for Automatic Detection of Brain Tumors in Magnetic Resonance Imaging Images," in IEEE Access, Vol. 10, pp. 2775-2782.

3. Perez Ursula; Estanislao Arana; David Moratal, Year: 2016, "Brain Metastases Detection Algorithms in Magnetic Resonance Imaging," *in* IEEE Latin America Transactions, Vol. 14, no. 3, pp. 1109-1114.

4. Thanh Dang Ngoc Hoang; Serdar Engínoğlu, Year: 2019 "An Iterative Mean Filter for Image Denoising," in IEEE Access, Vol. 7, pp. 167847-167859.

5. Borole Vipin Y; Sunil S. Nimbhore; Seema S. Kawthekar, Year: 2015, "Image processing techniques for brain tumor detection: A review." International Journal of Emerging Trends & Technology in Computer Science (IJETTCS), Vol. 4, no. 5.

6. Dhanachandra Nameirakpam; Khumanthem Manglem; Yambem Jina Chanu, Year: 2015, "Image segmentation using K-means clustering algorithm and subtractive clustering algorithm", Procedia Computer Science, Vol. 54, pp.764-771.

7. Huang Chunyan; Xiaorui Li; Yunliang Wen, Year: 2021, "AN OTSU image segmentation based on fruit fly optimization algorithm", Alexandria Engineering Journal, Vol. 60, no. 1, pp.183-188.

8. Jiang Junjun; Jiayi Ma; Chen Chen; Zhongyuan Wang; Zhihua Cai; Lizhe Wang, Year: 2018, "Super PCA: A Superpixelwise PCA Approach for Unsupervised Feature Extraction of Hyperspectral Imagery," *in* IEEE Transactions on Geoscience and Remote Sensing, Vol. 56, no. 8, pp. 4581-4593.

9. Feng Yingying, Year: 2020, "Mobile Terminal Video Image Fuzzy Feature Extraction Simulation Based on SURF Virtual Reality Technology," *in* IEEE Access, Vol. 8, pp. 156740-156751.

10. Yuan Shuai; Yanan Sun; Weifeng He; Qianrong Gu; Shi Xu; Zhigang Mao; Shikui Tu, Year: 2022, "MSLM-RF: A Spatial Feature Enhanced Random Forest for On-Board Hyperspectral Image Classification," in IEEE Transactions on Geoscience and Remote Sensing, Vol. 60, pp. 1-17.

11. Rahman Md Mahmudur; Sameer K. Antani; George R Thoma, Year: 2011, "A Learning-Based Similarity Fusion and Filtering Approach for Biomedical Image Retrieval Using SVM Classification

and Relevance Feedback," *in* IEEE Transactions on Information Technology in Biomedicine, Vol. 15, no. 4, pp. 640-646.

12. Zhang Yue; Jiong Wu; Yilong Liu; Yifan Chen; Ed X. Wu; Xiaoying Tang, Year: 2020, “MI-UNet: Multi-Inputs UNet Incorporating Brain Parcellation for Stroke Lesion Segmentation From T1-Weighted Magnetic Resonance Images”, in IEEE Journal of Biomedical and Health Informatics, Vol: 25, no: 02, pp: 526-535.

13. Zhou Yongjin; Weijian Huang; Pei Dong; Yong Xia; Shanshan Wang, Year: 2019, “D-UNet: A Dimension-Fusion U Shape Network for Chronic Stroke Lesion Segmentation”, in IEEE/ACM Transactions on Computational Biology and Bioinformatics, Vol: 18, no: 03, pp: 940-950.

14. Lee Hyunkwang; Yune Sehyo; Mansouri Mohammad; Kim Myeongchan; Tajmir Shahein; Guerrier Claude; Ebert Sarah; Pomerantz Stuart Romero; Javier Kamalian Shahmir; Gonzalez Ramon; Year: 2019, “An explainable deep-learning algorithm for the detection of acute intracranial haemorrhage from small datasets”, Nature Biomedical Engineering, Vol. 3, no. 3, pp. 173-182.

15. Hssayeni Murtadha D; Muayad S. Croock; Aymen D. Salman; Hassan F. Al-khafaji; Zakaria A. Yahya; Behnaz Ghoraani, Year: 2020. "Intracranial Hemorrhage Segmentation Using a Deep Convolutional Model”, no: 01.pp.4.

16. Liu Xinfeng; Hao Yang; Kehan Qi; Pei Dong; Qiegen Liu; Xin Liu; Rongpin Wang; Shanshan Wang, Year: 2019, “MSDF-Net: Multi-Scale Deep Fusion Network for Stroke Lesion Segmentation”, in IEEE Access, Vol: 07, pp: 178486-178495.